

Enhancing Multimodal Large Language Models with Vision Detection Models: An Empirical Study

Qirui Jiao¹ Daoyuan Chen² Yilun Huang² Yaliang Li² Ying Shen¹

Abstract

Despite the impressive capabilities of Multimodal Large Language Models (MLLMs) in integrating text and image modalities, challenges remain in accurately interpreting detailed visual elements. This paper presents an empirical study on enhancing MLLMs with state-of-the-art (SOTA) object detection and Optical Character Recognition models to improve fine-grained image understanding and reduce hallucination in responses. Our research investigates the embedding-based infusion of detection information, the impact of such infusion on the MLLMs’ original abilities, and the interchangeability of detection models. We conduct systematic experiments with models such as LLaVA-1.5, DINO, and PaddleOCRv2, revealing that our approach not only refines MLLMs’ performance in specific visual tasks but also maintains their original strengths. The resulting enhanced MLLMs outperform SOTA models on 9 out of 10 benchmarks, achieving an improvement of up to 12.99% on the normalized average score, marking a notable advancement in multimodal understanding. We release our codes to facilitate further exploration into the fine-grained multimodal dialogue capabilities of MLLMs.

1. Introduction

The advent of large language models (LLMs) has marked a new epoch in natural language processing (Brown et al., 2020; Touvron et al., 2023), laying the groundwork for the evolution of Multimodal Large Language Models (MLLMs) that blend linguistic and visual understanding. Pioneers such as GPT4V have led the charge, showcasing remarkable proficiency in numerous tasks (Yang et al., 2023). Despite their successes, a gap remains in these models’ ability to discern and accurately respond to queries about fine details

within images (Fu et al., 2023). This shortfall is particularly evident when MLLMs generate responses that are coherent yet misaligned with the image content, a phenomenon often referred to as “hallucination” (Li et al., 2023b).

Drawing parallels to human communication, where specificity in referencing objects is key to clarity, MLLMs stand to gain from improved precision in identifying objects and texts within images. To this end, one promising yet under-explored research direction is to leverage state-of-the-art (SOTA) object detection and Optical Character Recognition (OCR) technologies to alleviate hallucination.

The prowess of contemporary object detection and OCR models in precisely delineating objects and texts within images is well-established and can encompass both content and spatial information (Zou et al., 2023; Liu et al., 2024). In this paper, we hypothesize that their outputs can serve as the foundation for improving MLLMs’ granular understanding of images, and investigate how to effectively integrate this information. Based on SOTA models including LLaVA-1.5 (Liu et al., 2023a), DINO (Zhang et al., 2022) and PaddleOCRv2 (Du et al., 2021), we systematically navigate through a series of extensive experimentation to address the following issues:

(1) Can detection information be directly inputted into MLLMs? A straightforward method to enhance MLLMs with detection information is to integrate the textual representation of detected targets directly into the model. We examine the potential of enhancing MLLMs by converting detection outputs into text embeddings and incorporating them into the model, leveraging the pre-existing language understanding from the underlying LLMs. Our empirical evaluation first focuses on this approach, where we concatenate the detection token embeddings to the image features from ViT (Dosovitskiy et al., 2020) and feed them into the LLaVA-1.5 model. Interestingly, the results reveal that while the 7B variant of LLaVA-1.5 shows modest gains, the 13B variant deteriorates with untrained direct infusion, underscoring the need for further model retraining.

(2) Does training with detection information harm MLLM’s original ability? As applying in-context learning on MLLMs results in excessively long input sequences, we

¹Sun Yat-Sen University, China ²Alibaba Group. Correspondence to: Yaliang Li <yaliang.li@alibaba-inc.com>, Ying Shen <sheny76@mail.sysu.edu.cn>.



Figure 1. Examples on which LLaVA-1.5-13B fails while our model with detection information (LAF-13B) succeeds. “Detection” indicates detection information after our processing. More examples are provided in Figure 5 of Appendix B.

are interested in employing a training-based methodology to infuse detection information into MLLMs instead. We empirically show that retraining LLaVA-1.5 with detected results from auxiliary models enriches performance, yet dependency on this new information can overshadow the MLLM’s innate ability to leverage ViT information. We further explore fine-tuning strategies and show how to effectively harmonize these capabilities.

(3) What would happen if we replace the detection models? The characteristics of leveraged detection models impact the effectiveness of detection infusion. We also examine the replacement of DINO with an open-set object detection model called GroundingDINO (Liu et al., 2023c). Empirical results show further enhancement on MLLMs, with the capability to dynamically align object detection with the context of user queries during inference. This result also underscores the robustness of the studied injection approach, as it remains fully functional and effective following the replacement of detection models.

As a result, our experiments provide several key insights and affirm the value of the detection models infusion, with our enhanced MLLMs significantly outperforming LLaVA-1.5 across 9 of 10 benchmarks, asserting a new standard in fine-grained image understanding compared to many SOTA MLLMs. Furthermore, as shown in Figure 1, our MLLM effectively reduces hallucination and showcases enhanced efficacy in counting and localization tasks. In the realm of OCR tasks, it can also generate more accurate responses. Additionally, our MLLM excels in acquiring intricate details by pinpointing specific targets. For example, if it locates a clock, it can provide more accurate time-related information.

Our contributions can be summarized as follows:

- We conduct a thorough empirical investigation for infusing both object detection and OCR models into MLLMs. We further explore the potential of open-set object detection models to enable question-driven detection and validate the sustained efficacy of our method following the substitution of detection models.
- Built upon the insights gained, we develop an optimized approach for fine-grained image understanding, which elevates LLaVA-1.5 with 12.99% and 11.76% overall improvements for 7B and 13B size respectively.
- Our code is publicly available at [link](#) to facilitate further research, which we hope to help pave the way for systems that engage in more nuanced and accurate multimodal dialogue.

2. Related Works

Multimodal Large Language Models (MLLMs) Traditional Large Language Models (LLMs) are primarily tailored for text processing (Zhao et al., 2023). To integrate visual information, modality bridging modules have been developed to reconcile the representational disparities between text and images (Yin et al., 2023). Commonly, three lightweight approaches are employed:

Firstly, learnable queries are used to distill information from image features, as in Flamingo’s (Alayrac et al., 2022) perceiver resampler and IDEFICS’s (Hugo et al., 2023) similar feature sampling from CLIP ViT features. BLIP-2 (Li et al., 2023c) utilizes learnable queries in conjunction with

a Q-Former module, while Qwen-VL (Bai et al., 2023) compresses visual features into a sequence of fixed length using a cross-attention layer. Secondly, projection-based interfaces are employed to bridge modalities. Noteworthy models like LLaVA (Liu et al., 2023b) and LLaVA-1.5 (Liu et al., 2023a) utilize simple linear layers and activation functions for embedding image features with small sizes of training data. Lastly, parameter-efficient tuning modules are utilized. LLaMA-Adapter (Zhang et al., 2023; Gao et al., 2023) introduces self-attention layers with zero gating, and LaVIN (Luo et al., 2023) employs modality-specific adapters. Among them, our experiments are based on the popular SOTA model, LLaVA-1.5, employing a two-layer MLP as the modality bridging module.

Enhancing Detection Capabilities for MLLMs For models processing images, the ability to detect and localize targets is crucial. To improve MLLMs’ detection capabilities, typically two methods are explored:

The first method expands the dataset with existing object detection and OCR data. InstructBLIP (Dai et al., 2023), an enhancement of BLIP-2, utilizes data from 26 datasets spanning 11 tasks, including OCR. Shikra (Chen et al., 2023b) integrates RefCOCO (Kazemzadeh et al., 2014) and PointQA (Mani et al., 2020), generating fine-tuning data with GPT-4 and Flickr30K (Plummer et al., 2015). LLaVA and SPHINX (Lin et al., 2023) compile hybrid instruction fine-tuning datasets encompassing RefCOCO, VG (Krishna et al., 2017), and OCR dataset OCRVQA (Mishra et al., 2019). PINK (Xuan et al., 2023) employs a bootstrapping method to cover a range of referential comprehension tasks.

The second method restructures the image encoder to extract region-level information. LION (Chen et al., 2023a) introduces the Vision Aggregator for feature aggregation. Honeybee (Cha et al., 2023) utilizes a deformable attention-based abstractor with initialized reference points for fine-grained detail capture. UReader (Ye et al., 2023) employs a shape-adaptive cropping module and learnable queries to process local image features. Vary (Wei et al., 2023) develops a dedicated image encoder to extract textual content. These methodologies can enhance the detection capabilities of MLLMs, but they usually require a considerable volume of data to train their supplementary modules.

Distinct from these works, our study does not aim to expand datasets or introduce new architectures. Instead, we use the same datasets as LLaVA-1.5 and employ off-the-shelf detection models like DINO (Zhang et al., 2022) and PaddleOCRv2 (Du et al., 2021) to provide real-time object and text recognition information. Furthermore, our approach is modular, allowing flexibility to replace the current detection models with more advanced ones without additional costs.

3. Investigation Methodology for Detection Models Infusion

3.1. Motivational Observation

Existing MLLMs often encounter difficulties in accurately detecting targets. Consider LLaVA-1.5 as an example; despite its exceptional performance across various vision-language tasks, it is not infallible. Figure 1 illustrates this point, showing an instance where LLaVA-1.5 miscounts a herd of sheep, identifying six sheep as five, which points to a limitation in its object counting capability. Furthermore, LLaVA-1.5 fails to detect a pedestrian on the street who is partially obscured by a utility pole, underscoring a weakness in its object localization proficiency. In another scenario, LLaVA-1.5 incorrectly recognizes the license plate number “87025” as “547”, revealing shortcomings in its text recognition functionality.

By contrast, SOTA object detection and OCR models demonstrate consistently superior performance in these tasks. As depicted in Figure 1, the output from our processing with these detection models yields precise “Detection” annotations that enhance the MLLMs’ understanding of images and improve their performance in multimodal tasks.

Motivated by the limitations of current MLLMs, we aim to explore the infusion of off-the-shelf detection models into MLLMs. The remainder of this section details our design for an extensive empirical investigation into effective fusion strategies. The results and analysis of this study are presented in the following Section 4.

3.2. Studied Model Architecture

In terms of the object detection model, we first choose the popular end-to-end model based on Transformer, DINO (Zhang et al., 2022), which gains SOTA performance across multiple object detection tasks. With DINO, we can extract information regarding the class labels and bounding box coordinates of identified objects. Specifically, we first convert the outputs of DINO to the textual format. To reduce the sentence length, we select the first two values from the bounding box coordinates as positional information, which represent the central coordinates of the corresponding objects. Then, we consolidate objects within the same category, further reducing the length while serving as a counter as well. Finally, as Figure 3 shown, we add an instruction (INS) sentence before the categories and coordinates description to combine the final result, whose text example looks like: “Here are the central coordinates of certain objects in this image: 2 person:[{0.25, 0.12}, [0.11, 0.43]], 1 cake:[{0.42, 0.32}].”

Moreover, we explore replacing DINO with an open-set

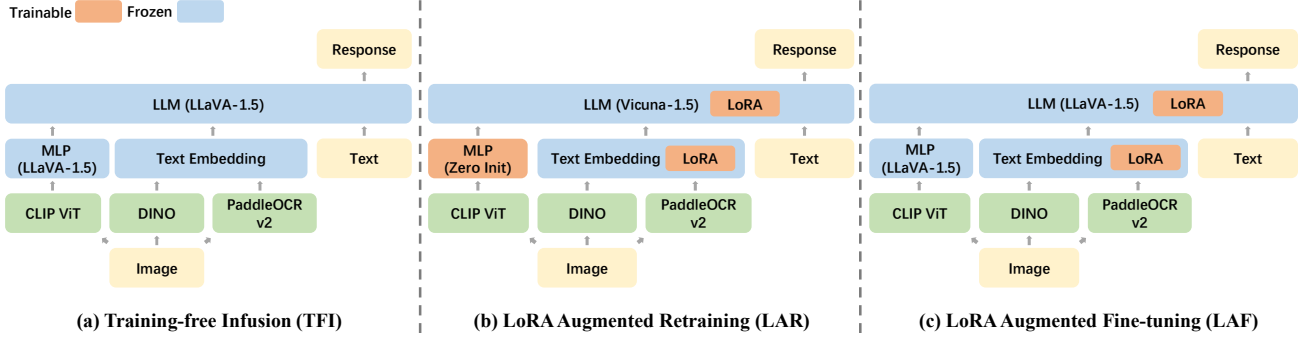


Figure 2. The illustration of investigated MLLM architectures with different strategies to infuse detection information.

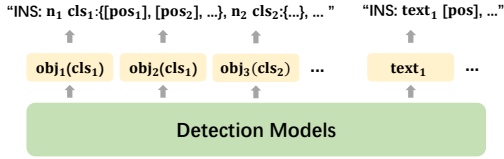


Figure 3. The composition of detection information. “INS”, “obj/cls” and “pos” indicate instruction, detected object/class name, and position text respectively. Specific examples are provided in Figure 6 of Appendix C.

object detection model called GroundingDINO (Liu et al., 2023c), aiming to assess whether our model can still work effectively after the substitution of detection models.

For the OCR information, we choose PaddleOCRv2 (Du et al., 2021), a lightweight OCR system designed for high text detection accuracy and efficiency. With PaddleOCRv2, we can acquire textual content within images along with their corresponding positional information. Similar to object detection, we process OCR results into a textual format, e.g., “Here are the central coordinates of certain texts in this image: ‘Birthday’ [0.41, 0.85], ‘YEARS’ [0.11, 0.34].”

In Appendix A, we conduct a statistical analysis on the length of detection information, revealing that the current method for constructing detection information effectively manages its length, mitigating the occurrence of excessively long sentences. Besides, specific examples with corresponding images are provided in Appendix C.

For the MLLMs, Figure 2 illustrates the overall architecture of our studied model in different settings. Based on the popular SOTA MLLM, LLaVA-1.5, we utilize CLIP-ViT-L-336px to extract the image-level features from images and employ a two-layer MLP to map these features into the semantic space of LLM. Subsequently, we separately use DINO and PaddleOCRv2 to obtain object detection and OCR results. These results are then transformed into

sentences using the methods mentioned above and converted into text features using the Embedding Layers of LLM. Next, we concatenate the image-level information and the detection information before feeding them into the backbone LLM. As a result, the MLLM can simultaneously obtain both the overall image information and the fine-grained image details during its training and inference stages.

3.3. Infusion Strategies

Besides the model architecture, the training process plays a vital role in enhancing MLLM’s capabilities to understand and utilize the supplementary detection information. We then design a series of experiments to identify effective fusion strategies in terms of model training.

Training-free Infusion (TFI) For the first fusion strategy, we directly feed the detection information into LLaVA-1.5 without any additional training. As shown in Figure 2(a), we use the same model structure and weights as LLaVA-1.5, with the only distinction being the incorporation of processed text from detection models and our concatenation operation (introduced in Section 3.2).

LoRA Augmented Retraining (LAR) For the second fusion strategy, we train the model from scratch as LLaVA-1.5. As shown in Figure 2(b), we first initialize the MLP module and pretrain it with LCS-558K datasets (Liu et al., 2023a) during the pretraining process. Subsequently, we introduce a LoRA (Hu et al., 2021) module into the following LLM Vicuna-1.5 (Chiang et al., 2023). After that, we train the LoRA module and MLP module during the instruction fine-tuning process with LLaVA-1.5’s instruction-following dataset. (The detailed information of this dataset is provided in Appendix D.) Throughout the entire training process, we consistently incorporate the detection information.

LoRA Augmented Fine-tuning (LAF) For the third fusion strategy, we attempt to conduct fine-tuning on LLaVA-1.5. As shown in Figure 2(c), we freeze the weights of both the MLP module and backbone LLM of LLaVA-1.5. Following this, we introduce a LoRA module to the LLM and train

the LoRA module for a single epoch with LLaVA-1.5’s instruction-following dataset, concurrently incorporating the detection information. (The training hyper-parameters of LAR and LAF are provided in Appendix E.)

3.4. Quantitative Evaluation Settings

We employ ten benchmarks to evaluate various MLLM capabilities. VQAv2 (Goyal et al., 2017), GQA (Hudson & Manning, 2019), and MME (Fu et al., 2023) measure *comprehensive VQA capabilities*; MMBench (Liu et al., 2023d) and SEED-Bench (Li et al., 2023a) test *perceptual and reasoning abilities*; TextVQA (Singh et al., 2019) assesses *text recognition*; MM-Vet (Yu et al., 2023) evaluates *complex task handling with local information*; and POPE (Li et al., 2023d) measures *detected object hallucination and fine-grained object localization*.

For a fair and more comprehensive comparison, we employ an aggregated score across all considered benchmarks. Specifically, we first normalize the score for each benchmark as $s_{norm} = (s - s_{min}) / (s_{max} - s_{min})$, where s denotes the original benchmark score, s_{min} and s_{max} refers to the lowest and highest score across all considered methods respectively. Subsequently, we compute the mean of s_{norm} across all benchmarks and denote it as \bar{s}_{norm} .

Due to the limited space in tables, benchmark names are abbreviated: VQA^{v2} as VQA-v2, VQA^T as TextVQA, MMB as MMBench, MMB^{CN} as MMBench-Chinese, SEED as SEED-Bench, MME^P as MME-Perception, and MME^C as MME-Cognition.

4. Main Results and Analysis

4.1. Lesson 1: Original MLLMs Struggle with Comprehending Detection Information

Initially, we don’t conduct any training on LLaVA-1.5. Instead, we directly feed the detection information into the model, aiming to observe whether the original LLaVA-1.5 can comprehend the detection information we input. We call this fusion strategy “Training-free Infusion” (TFI) as mentioned in Section 3.3.

As presented in Table 1, *TFI-7B exhibits partial enhancement in some benchmarks, while TFI-13B shows a discernible decline*. Simultaneously, both models show significant improvement on the POPE benchmark, which evaluates object hallucination, indicating that the supplementary object detection information exerts a positive influence. Additionally, they exhibit robust performance on the MME-Cognition benchmark, which encompasses numerous questions related to text within images, suggesting the OCR information is also demonstrating efficacy.

However, other benchmarks exhibit fluctuations in scores,

Method	VQA ^{v2}	GQA	VQA ^T	POPE	MME ^P
LLaVA-1.5-7B	78.5	62.0	58.2	85.9	1510.7
TFI-7B	78.5	60.7 ↓	59.2 ↑	89.9 ↑	1497.0 ↓
LLaVA-1.5-13B	80.0	63.3	61.3	85.9	1531.3
TFI-13B	76.6 ↓	60.2 ↓	59.6 ↓	88.3 ↑	1453.6 ↓
	MME ^C	MMB	MMB ^{CN}	MM-Vet	SEED
LLaVA-1.5-7B	355.7	64.3	58.3	30.5	58.6
TFI-7B	401.0 ↑	65.0 ↑	57.2 ↓	33.7 ↑	60.6 ↑
LLaVA-1.5-13B	295.4	67.7	63.6	35.4	61.6
TFI-13B	401.0 ↑	65.0 ↓	57.5 ↓	31.7 ↓	60.7 ↓

Table 1. Comparison between “Training-free Infusion” (TFI) models and LLaVA-1.5 across 10 benchmarks.

Method	VQA ^{v2}	GQA	VQA ^T	POPE	MME ^P
LLaVA-1.5-7B	78.5	62.0	58.2	85.9	1510.7
LAR-7B	78.5	57.7 ↓	60.0 ↑	89.3 ↑	1454.5 ↓
LLaVA-1.5-13B	80.0	63.3	61.3	85.9	1531.3
LAR-13B	79.2 ↓	59.0 ↓	61.7 ↑	89.2 ↑	1491.2 ↓
	MME ^C	MMB	MMB ^{CN}	MM-Vet	SEED
LLaVA-1.5-7B	355.7	64.3	58.3	30.5	58.6
LAR-7B	412.0 ↑	66.2 ↑	60.6 ↑	31.5 ↑	60.8 ↑
LLaVA-1.5-13B	295.4	67.7	63.6	35.4	61.6
LAR-13B	409.6 ↑	69.5 ↑	63.2 ↓	35.1 ↓	62.5 ↑

Table 2. Comparison between “LoRA Augmented Retraining” (LAR) models and LLaVA-1.5 across 10 benchmarks.

implying a deficiency in our model’s utilization of detection information. Upon closer analysis, we speculate that the infusion of detection information introduces extraneous content. In the absence of proper training, there is a tendency for MLLMs to interpret this noise as pertinent information, thereby adversely affecting the accuracy of inference. Consequently, we need to conduct additional training on the model to enhance its proficiency in extracting valuable information from supplementary detection information and eliminating noise.

4.2. Lesson 2: Detection Re-Training has Adverse Effects on Comprehending ViT Features

Researchers commonly employ in-context learning (ICL) (Dong et al., 2022) to instruct LLMs in the recognition of specific input formats. However, for MLLMs, ICL becomes difficult as it necessitates processing lengthy input sequences combining image features in tokens format. Therefore, we opt against using ICL for MLLMs in favor of a training-based approach, and shifting into the second fusion strategy mentioned in Section 3.3, “LoRA Augmented Retraining” (LAR). In this strategy, we retrain LLaVA-1.5 with its original training strategy, concurrently incorporating the detection information.

As shown in Table 2, *LAR models outperform LLaVA-1.5*

Method	VQA ^{v2}	GQA	VQA ^T	POPE	MME ^P
LLaVA-1.5-7B	78.5	62.0	58.2	85.9	1510.7
LAR-7B w/o DI	76.4 ↓	56.8 ↓	56.6 ↓	85.5 ↓	1387.7 ↓
LLaVA-1.5-13B	80.0	63.3	61.3	85.9	1531.3
LAR-13B w/o DI	77.3 ↓	58.0 ↓	58.2 ↓	83.4 ↓	1442.6 ↓
	MME ^C	MMB	MMB ^{CN}	MM-Vet	SEED
LLaVA-1.5-7B	355.7	64.3	58.3	30.5	58.6
LAR-7B w/o DI	312.5 ↓	65.5 ↑	58.3	29.0 ↓	59.6 ↑
LLaVA-1.5-13B	295.4	67.7	63.6	35.4	61.6
LAR-13B w/o DI	310.7 ↑	68.5 ↑	61.7 ↓	30.6 ↓	61.6 ↑

Table 3. Performance of “LoRA Augmented Retraining” (LAR) models without detection information (w/o DI).

on multiple benchmarks. Notably, they show a 4% improvement on the POPE benchmark, which assesses object hallucination. Additionally, they show significant improvements in MME-cognition and TextVQA, which are related to text recognition. Furthermore, they also show improvements in the MMBench and Seed-Bench.

However, LAR models do not show improvement across all benchmarks. On VQAv2, GQA, and MME, there is a noticeable decline. Nevertheless, as we employ identical model architecture and datasets as LLaVA-1.5, our model’s performance is expected to be on par with, if not superior to, that of LLaVA-1.5. Since LLaVA-1.5 exclusively employs ViT for image feature extraction, we speculate that the infusion of detection information during training has a negative effect on the model’s ability to learn how to utilize features from ViT. As we know, the evaluation datasets encompass a substantial amount of samples that do not require fine-grained information but rather demand image-level information. Upon these samples, the model places greater reliance on ViT features. Therefore, while facilitating the model’s learning of how to utilize detection information, it is crucial to simultaneously ensure the model preserves its capability to leverage ViT features.

Thus, we then evaluate the performance of LAR models with no detection information applied. In this way, their benchmark scores are only related to the features from ViT. The results are presented in Table 3, which show a noticeable performance lag compared to LLaVA-1.5, suggesting that *integrating detection information during training does impact MLLM in learning how to use the image features extracted from ViT*. The current MLLMs fail to learn how to appropriately prioritize the ViT features and detection information, calling for further improved fusion strategies.

4.3. Lesson 3: Suitable Fine-tuning Achieves Good Trade-off for Detection Infusion

Retraining could inevitably pose challenges for the model in precisely evaluating the significance of ViT features and de-

tection information, thereby causing a performance decline on tasks unrelated to detection. To enhance the model’s ability to make well-informed trade-offs between these two types of information, for the third fusion strategy, we decide to leverage the well-trained parameters of LLaVA-1.5 and fine-tune our models based on its original weights. We call this fusion strategy “LoRA Augmented Fine-tuning”, abbreviated as LAF.

As shown in Table 4, *both the 7B and 13B models of LAF exhibit superior performance compared to LLaVA-1.5*. Simultaneously, as indicated in Appendix H, the current models demonstrate significant improvement in comparison to the retraining models, indicating that *the fine-tuning strategy effectively makes trade-offs between ViT features and detection information*.

Upon detailed analysis, we find that LAF models exhibit a visible improvement on comprehensive VQA benchmarks such as VQAv2 and MME. On the benchmarks that evaluate perceptual and reasoning abilities, such as MMBench and SEED-Bench, the models’ performance undergoes a noticeable enhancement. Additionally, the infusion of object detection information yields a substantial enhancement in performance on both the POPE benchmark, assessing object hallucinations, and the MM-Vet benchmark, gauging the ability to exploit local information. Due to the incorporation of OCR information, the models also exhibit commendable performance on text-related benchmarks such as TextVQA and MME-cognition. Finally, on the aggregated performance measure \bar{s}_{norm} , LAF models unequivocally outperform LLaVA-1.5 and other considered SOTA models, demonstrating the significant efficacy of our approach.

Nevertheless, our models exhibit a noticeable performance decline on the GQA benchmark. Upon closer examination, we consider that the decrease is linked to the supplementary detection information. Since we use category names to identify detected objects, the model tends to use these category names to recognize the specific objects. For example, if our model responds with “car” instead of the ground truth answer “SUV”, it could lead to inaccuracies.

In Figure 1, we compare the performance of LAF-13B with LLaVA-1.5-13B, providing examples on which LLaVA-1.5 produces incorrect answers while our model yields correct responses (more examples are in Appendix B). With object detection information, our model effectively achieves precise counts and delineates the respective positions of specified objects. With OCR information, our model proficiently generates textual content in response to the localization requirements outlined in questions. Furthermore, it is observed that our model can use the object detection information to refine its comprehension of the information conveyed by particular objects. For instance, when the model discerns the location of a clock within the image, it

Enhancing Multimodal Large Language Models with Vision Detection Models

Method	LLM	VQA ^{v2}	GQA	VQA ^T	POPE	MME	MMB	MMB ^{CN}	MM-Vet	SEED	\bar{s}_{norm}
BLIP-2	Vicuna-13B	41.0	41.0	42.5	85.3	1583.8	-	-	22.4	46.4	0.17
InstructBLIP	Vicuna-13B	-	49.5	50.7	78.9	1504.6	-	-	25.6	-	0.24
LLaMA-AdapterV2	LLaMA-65B	70.7	45.1	37.4	-	1684.8	-	-	-	-	0.39
IDEFICS-80B	LLaMA-65B	60.0	45.2	30.9	-	-	54.5	38.1	-	-	0.34
Qwen-VL	Qwen-7B	78.8	59.3	63.8	-	-	38.2	7.4	-	56.3	0.54
Qwen-VL-Chat	Qwen-7B	78.2	57.5	61.5	-	1848.2	60.6	56.7	-	58.2	0.78
SPHINX	LLaMA2-13B	78.1	<u>62.6</u>	51.6	80.7	1798.3	66.9	56.2	<u>36.0</u>	69.1	0.77
LLaVA-1.5-7B	Vicuna-1.5-7B	78.5	62.0	58.2	85.9	1866.4	64.3	58.3	30.5	58.6	0.77
LAR-7B (our)	Vicuna-1.5-7B	78.5	57.7 \downarrow	60.0 \uparrow	89.3 \uparrow	1866.5 \uparrow	66.2 \uparrow	60.6 \uparrow	31.5 \uparrow	60.8 \uparrow	0.82 \uparrow
LAF-7B (our)	LLaVA-1.5-7B	79.0 \uparrow	60.5 \downarrow	60.1 \uparrow	88.9 \uparrow	1880.5 \uparrow	67.3 \uparrow	60.2 \uparrow	35.2 \uparrow	60.8 \uparrow	0.87 \uparrow
LLaVA-1.5-13B	Vicuna-1.5-13B	<u>80.0</u>	63.3	61.3	85.9	1826.7	67.7	<u>63.6</u>	35.4	61.6	0.85
LAR-13B (our)	Vicuna-1.5-13B	79.2 \downarrow	59.0 \downarrow	61.7 \uparrow	89.2 \uparrow	<u>1900.9 \uparrow</u>	<u>69.5 \uparrow</u>	63.2 \downarrow	35.1 \downarrow	<u>62.5 \uparrow</u>	0.89 \uparrow
LAF-13B (our)	LLaVA-1.5-13B	80.3 \uparrow	62.2 \downarrow	<u>61.8 \uparrow</u>	<u>88.8 \uparrow</u>	1920.5 \uparrow	71.4 \uparrow	65.2 \uparrow	38.9 \uparrow	62.3 \uparrow	0.95 \uparrow

Table 4. Comparison between “LoRA Augmented Retraining” (LAR) models, “LoRA Augmented Fine-tuning” (LAF) models, and SOTA methods on 10 benchmarks. Our LAF approach effectively infuses detection information into LLaVA-1.5, leading to a considerable performance enhancement across 9/10 benchmarks. \bar{s}_{norm} is an aggregated performance measure across all considered benchmarks. MME represents the summation of MME^P and MME^C, with detailed information provided in Appendix F.



Figure 4. Examples on which LLaVA-1.5 fails while our model with open-set object detection information succeeds.

can more effectively extract the displayed content on the clock, thereby acquiring the correct time.

In Appendix G, we fine-tune another version of LLaVA-1.5 without the addition of detection information, indicating that the exceptional performance of LAF models is primarily ascribed to the supplementary detection information, rather than the additional fine-tuning conducted on LLaVA-1.5. Besides, in Appendix I, we show the model’s performance on leveraging object detection information and OCR information separately.

4.4. Lesson 4: Detection Models Can be Flexibly and Effectively Replaced

In the previous experiments, we employ DINO to extract object detection information and successfully facilitate per-

formance improvement for MLLMs. However, it is essential to note that DINO is a closed-set object detection model, capable of detecting only 90 common object categories. Nevertheless, images may contain uncommon objects or specific entities such as certain celebrities or objects with attributive modifiers. In such scenarios, the closed-set object detection models exhibit limitations in efficacy.

Fortunately, our model is modular, which means that we have the flexibility to replace the embedded detection models. Thus, in this experiment, we will substitute the detection model to observe whether, after the replacement, our model can still operate effectively.

We introduce an open-set object detection model called GroundingDINO (Liu et al., 2023c). GroundingDINO is designed to detect objects related to input text. With this

model, our model can precisely pinpoint the targets by referencing the object names mentioned in the questions. To achieve this, we extract target names from the input questions, subsequently concatenating them to create prompts. After that, GroundingDINO follows the prompts to generate location information for the corresponding targets. Finally, we convert the outputs into the sentence format preconceived in our design, with subsequent steps aligning with those employed during the DINO usage process.

In Figure 4, we enumerate cases where LLaVA-1.5 provides incorrect answers while our model with open-set object detection information produces correct responses. With this information, our model can carry out counting tasks and object localization tasks more purposefully, as it can leverage the target names in questions to get specific positional information. As shown in Figure 3, our model can precisely count the number of “blue guitars” or “SUVs” in images, all of which are specialized nouns that DINO cannot deal with. Besides, our model can also accurately locate specific targets, such as “a brown horse” and “the monkey doll”. Furthermore, by acquiring detection information that is linked to the specific targets, the model improves its precision in capturing relevant details associated with them. For instance, in Figure 4, our model accurately distinguishes the driving direction of the blue taxi, whereas LLaVA-1.5-13B fails.

To sum up, with open-set object detection, our model can successfully deal with targets not included in closed-set object detection, thereby expanding the applicability. Moreover, *after directly replacing DINO with GroundingDINO, our model continues to operate effectively*, which indicates that directly substituting the detection models is feasible and we have the flexibility to replace the detection models as needed. Hence, thanks to our model framework and training methodology, when there are superior detection models available in the future, we can directly incorporate them to enhance the performance of our model.

4.5. Discussions

In light of our empirical findings, potential enhancements to our MLLM framework with integrated vision detection capabilities have emerged. These insights pave the way for future research avenues that can further refine the model’s performance and applicability.

Refinement of Detection Models: The success of our model relies heavily on the accuracy and reliability of the underlying object and OCR detection models. Closed-set object detection models are highly efficient within their predefined categories yet are constrained by their limited scope. Open-set models offer a more expansive range but can be prone to inaccuracies. Similarly, OCR models are susceptible to errors in text recognition. Future work could explore the development and integration of more sophisticated detec-

tion models that exhibit a wider detection range while maintaining high accuracy. Advancements in zero-shot learning and few-shot learning could also be incorporated to enhance the model’s ability to generalize from limited examples and improve detection in open-set scenarios.

Enhanced Model Utilization of Detection Information:

The experiments have shown that there are circumstances where our model does not effectively utilize the positional information provided by the detection models. This suggests a potential gap in the model’s ability to integrate visual cues with textual information fully. Investigating novel training methodologies or architectural modifications that can better inform the model about the utility of detection features is an exciting area of research. For instance, attention mechanisms could be refined to give the model more nuanced control over how it incorporates visual and textual features, or new loss functions could be designed to incentivize the model to leverage detection outputs more effectively.

Robustness to Detection Errors: Building robustness to inaccuracies in detection models is critical for real-world applications. Future iterations of our framework could include mechanisms to identify and mitigate the impact of detection errors on the model’s outputs. Error detection algorithms, confidence estimation techniques, or incorporating human-in-the-loop validation are potential strategies to enhance the model’s robustness.

5. Conclusion

In this paper, we systematically conduct a series of experiments to find the most effective fusion strategy for integrating SOTA object detection and OCR models into MLLMs. After thorough investigation, we determine that fine-tuning for a single epoch on original LLaVA-1.5, along with the simultaneous integration of detection information during training, proves to be the most effective approach. Moreover, we replace the detection model from DINO to GroundingDINO and observe that the updated model demonstrates continued proper functionality. This highlights the modular structure of our model, demonstrating its capability to stay abreast of evolving object detection technologies and gain sustained enhancement of performance.

In a nutshell, we provide a series of progressive insights about the effective infusion of supplementary object detection and OCR information for MLLMs, and derive models that exhibit exceptional performance over SOTA MLLMs in various tasks such as counting, object localization, and text recognition. With this work, we hope it can benefit future MLLM research and development that approaches better understanding, interpreting and engaging with fine-grained multimodal content.

References

- Alayrac, J.-B., Donahue, J., Luc, P., Miech, A., Barr, I., Hasson, Y., Lenc, K., Mensch, A., Millican, K., Reynolds, M., et al. Flamingo: a visual language model for few-shot learning. *Advances in Neural Information Processing Systems*, 35:23716–23736, 2022.
- Bai, J., Bai, S., Yang, S., Wang, S., Tan, S., Wang, P., Lin, J., Zhou, C., and Zhou, J. Qwen-vl: A frontier large vision-language model with versatile abilities. *arXiv preprint arXiv:2308.12966*, 2023.
- Brown, T., Mann, B., Ryder, N., Subbiah, M., Kaplan, J. D., Dhariwal, P., Neelakantan, A., Shyam, P., Sastry, G., Askell, A., et al. Language models are few-shot learners. *Advances in neural information processing systems*, 33: 1877–1901, 2020.
- Cha, J., Kang, W., Mun, J., and Roh, B. Honeybee: Locality-enhanced projector for multimodal llm. *arXiv preprint arXiv:2312.06742*, 2023.
- Chen, G., Shen, L., Shao, R., Deng, X., and Nie, L. Lion: Empowering multimodal large language model with dual-level visual knowledge. *arXiv preprint arXiv:2311.11860*, 2023a.
- Chen, K., Zhang, Z., Zeng, W., Zhang, R., Zhu, F., and Zhao, R. Shikra: Unleashing multimodal llm’s referential dialogue magic. *arXiv preprint arXiv:2306.15195*, 2023b.
- Chiang, W.-L., Li, Z., Lin, Z., Sheng, Y., Wu, Z., Zhang, H., Zheng, L., Zhuang, S., Zhuang, Y., Gonzalez, J. E., et al. Vicuna: An open-source chatbot impressing gpt-4 with 90%* chatgpt quality. See <https://vicuna.lmsys.org> (accessed 14 April 2023), 2023.
- Dai, W., Li, J., Li, D., Tiong, A., Zhao, J., Wang, W., Li, B., Fung, P., and Hoi, S. Instructblip: Towards general-purpose vision-language models with instruction tuning. *arXiv preprint arXiv:2305.06500*, 2023.
- Dong, Q., Li, L., Dai, D., Zheng, C., Wu, Z., Chang, B., Sun, X., Xu, J., and Sui, Z. A survey for in-context learning. *arXiv preprint arXiv:2301.00234*, 2022.
- Dosovitskiy, A., Beyer, L., Kolesnikov, A., Weissenborn, D., Zhai, X., Unterthiner, T., Dehghani, M., Minderer, M., Heigold, G., Gelly, S., et al. An image is worth 16x16 words: Transformers for image recognition at scale. *arXiv preprint arXiv:2010.11929*, 2020.
- Du, Y., Li, C., Guo, R., Cui, C., Liu, W., Zhou, J., Lu, B., Yang, Y., Liu, Q., Hu, X., et al. Pp-ocrv2: Bag of tricks for ultra lightweight ocr system. *arXiv preprint arXiv:2109.03144*, 2021.
- Fu, C., Chen, P., Shen, Y., Qin, Y., Zhang, M., Lin, X., Yang, J., Zheng, X., Li, K., Sun, X., et al. Mme: A comprehensive evaluation benchmark for multimodal large language models. *arXiv preprint arXiv:2306.13394*, 2023.
- Gao, P., Han, J., Zhang, R., Lin, Z., Geng, S., Zhou, A., Zhang, W., Lu, P., He, C., Yue, X., et al. Llama-adapter v2: Parameter-efficient visual instruction model. *arXiv preprint arXiv:2304.15010*, 2023.
- Goyal, Y., Khot, T., Summers-Stay, D., Batra, D., and Parikh, D. Making the v in vqa matter: Elevating the role of image understanding in visual question answering. In *Proceedings of the IEEE conference on computer vision and pattern recognition*, pp. 6904–6913, 2017.
- Hu, E. J., Shen, Y., Wallis, P., Allen-Zhu, Z., Li, Y., Wang, S., Wang, L., and Chen, W. Lora: Low-rank adaptation of large language models. *arXiv preprint arXiv:2106.09685*, 2021.
- Hudson, D. A. and Manning, C. D. Gqa: A new dataset for real-world visual reasoning and compositional question answering. In *Proceedings of the IEEE/CVF conference on computer vision and pattern recognition*, pp. 6700–6709, 2019.
- Hugo, L., Daniel, v. S., Stas, B., Leo, T., Lucile, S., Thomas, W., Siddharth, K., Amanpreet, S., Giada, P., Yacine, J., and Victor, S. Introducing idefics: An open reproduction of state-of-the-art visual language model. <https://huggingface.co/blog/idefics>, 2023.
- Kazemzadeh, S., Ordonez, V., Matten, M., and Berg, T. Referitgame: Referring to objects in photographs of natural scenes. In *Proceedings of the 2014 conference on empirical methods in natural language processing (EMNLP)*, pp. 787–798, 2014.
- Krishna, R., Zhu, Y., Groth, O., Johnson, J., Hata, K., Kravitz, J., Chen, S., Kalantidis, Y., Li, L.-J., Shamma, D. A., et al. Visual genome: Connecting language and vision using crowdsourced dense image annotations. *International journal of computer vision*, 123:32–73, 2017.
- Li, B., Wang, R., Wang, G., Ge, Y., Ge, Y., and Shan, Y. Seed-bench: Benchmarking multimodal llms with generative comprehension. *arXiv preprint arXiv:2307.16125*, 2023a.
- Li, C., Gan, Z., Yang, Z., Yang, J., Li, L., Wang, L., and Gao, J. Multimodal foundation models: From specialists to general-purpose assistants. *arXiv preprint arXiv:2309.10020*, 1(2):2, 2023b.
- Li, J., Li, D., Savarese, S., and Hoi, S. Blip-2: Bootstrapping language-image pre-training with frozen image encoders and large language models. *arXiv preprint arXiv:2301.12597*, 2023c.

- Li, Y., Du, Y., Zhou, K., Wang, J., Zhao, W. X., and Wen, J.-R. Evaluating object hallucination in large vision-language models. *arXiv preprint arXiv:2305.10355*, 2023d.
- Lin, Z., Liu, C., Zhang, R., Gao, P., Qiu, L., Xiao, H., Qiu, H., Lin, C., Shao, W., Chen, K., et al. Sphinx: The joint mixing of weights, tasks, and visual embeddings for multi-modal large language models. *arXiv preprint arXiv:2311.07575*, 2023.
- Liu, H., Li, C., Li, Y., and Lee, Y. J. Improved baselines with visual instruction tuning. *arXiv preprint arXiv:2310.03744*, 2023a.
- Liu, H., Li, C., Wu, Q., and Lee, Y. J. Visual instruction tuning. *arXiv preprint arXiv:2304.08485*, 2023b.
- Liu, S., Zeng, Z., Ren, T., Li, F., Zhang, H., Yang, J., Li, C., Yang, J., Su, H., Zhu, J., et al. Grounding dino: Marrying dino with grounded pre-training for open-set object detection. *arXiv preprint arXiv:2303.05499*, 2023c.
- Liu, Y., Duan, H., Zhang, Y., Li, B., Zhang, S., Zhao, W., Yuan, Y., Wang, J., He, C., Liu, Z., et al. Mmbench: Is your multi-modal model an all-around player? *arXiv preprint arXiv:2307.06281*, 2023d.
- Liu, Y., Li, Z., Yang, B., Li, C., Yin, X., Lin Liu, C., Jin, L., and Bai, X. On the hidden mystery of ocr in large multimodal models, 2024.
- Luo, G., Zhou, Y., Ren, T., Chen, S., Sun, X., and Ji, R. Cheap and quick: Efficient vision-language instruction tuning for large language models. *arXiv preprint arXiv:2305.15023*, 2023.
- Mani, A., Yoo, N., Hinthorn, W., and Russakovsky, O. Point and ask: Incorporating pointing into visual question answering. *arXiv preprint arXiv:2011.13681*, 2020.
- Marino, K., Rastegari, M., Farhadi, A., and Mottaghi, R. Ok-vqa: A visual question answering benchmark requiring external knowledge. In *Proceedings of the IEEE/cvf conference on computer vision and pattern recognition*, pp. 3195–3204, 2019.
- Mishra, A., Shekhar, S., Singh, A. K., and Chakraborty, A. Ocr-vqa: Visual question answering by reading text in images. In *2019 international conference on document analysis and recognition (ICDAR)*, pp. 947–952. IEEE, 2019.
- Plummer, B. A., Wang, L., Cervantes, C. M., Caicedo, J. C., Hockenmaier, J., and Lazebnik, S. Flickr30k entities: Collecting region-to-phrase correspondences for richer image-to-sentence models. In *Proceedings of the IEEE international conference on computer vision*, pp. 2641–2649, 2015.
- Schwenk, D., Khandelwal, A., Clark, C., Marino, K., and Mottaghi, R. A-okvqa: A benchmark for visual question answering using world knowledge. In *European Conference on Computer Vision*, pp. 146–162. Springer, 2022.
- Sidorov, O., Hu, R., Rohrbach, M., and Singh, A. Textcaps: a dataset for image captioning with reading comprehension. In *Computer Vision—ECCV 2020: 16th European Conference, Glasgow, UK, August 23–28, 2020, Proceedings, Part II 16*, pp. 742–758. Springer, 2020.
- Singh, A., Natarajan, V., Shah, M., Jiang, Y., Chen, X., Batra, D., Parikh, D., and Rohrbach, M. Towards vqa models that can read. In *Proceedings of the IEEE/CVF conference on computer vision and pattern recognition*, pp. 8317–8326, 2019.
- Touvron, H., Lavril, T., Izacard, G., Martinet, X., Lachaux, M.-A., Lacroix, T., Rozière, B., Goyal, N., Hambro, E., Azhar, F., et al. Llama: Open and efficient foundation language models. *arXiv preprint arXiv:2302.13971*, 2023.
- Wei, H., Kong, L., Chen, J., Zhao, L., Ge, Z., Yang, J., Sun, J., Han, C., and Zhang, X. Vary: Scaling up the vision vocabulary for large vision-language models. *arXiv preprint arXiv:2312.06109*, 2023.
- Xuan, S., Guo, Q., Yang, M., and Zhang, S. Pink: Unveiling the power of referential comprehension for multi-modal llms. *arXiv preprint arXiv:2310.00582*, 2023.
- Yang, Z., Li, L., Lin, K., Wang, J., Lin, C.-C., Liu, Z., and Wang, L. The dawn of llms: Preliminary explorations with gpt-4v (ision). *arXiv preprint arXiv:2309.17421*, 9 (1):1, 2023.
- Ye, J., Hu, A., Xu, H., Ye, Q., Yan, M., Xu, G., Li, C., Tian, J., Qian, Q., Zhang, J., et al. Ureader: Universal ocr-free visually-situated language understanding with multimodal large language model. *arXiv preprint arXiv:2310.05126*, 2023.
- Yin, S., Fu, C., Zhao, S., Li, K., Sun, X., Xu, T., and Chen, E. A survey on multimodal large language models. *arXiv preprint arXiv:2306.13549*, 2023.
- Yu, W., Yang, Z., Li, L., Wang, J., Lin, K., Liu, Z., Wang, X., and Wang, L. Mm-vet: Evaluating large multimodal models for integrated capabilities. *arXiv preprint arXiv:2308.02490*, 2023.
- Zhang, H., Li, F., Liu, S., Zhang, L., Su, H., Zhu, J., Ni, L. M., and Shum, H.-Y. Dino: Detr with improved denoising anchor boxes for end-to-end object detection. *arXiv preprint arXiv:2203.03605*, 2022.

Zhang, R., Han, J., Zhou, A., Hu, X., Yan, S., Lu, P., Li, H., Gao, P., and Qiao, Y. Llama-adapter: Efficient fine-tuning of language models with zero-init attention. *arXiv preprint arXiv:2303.16199*, 2023.

Zhao, W. X., Zhou, K., Li, J., Tang, T., Wang, X., Hou, Y., Min, Y., Zhang, B., Zhang, J., Dong, Z., Du, Y., Yang, C., Chen, Y., Chen, Z., Jiang, J., Ren, R., Li, Y., Tang, X., Liu, Z., Liu, P., Nie, J.-Y., and Wen, J.-R. A survey of large language models, 2023.

Zou, Z., Chen, K., Shi, Z., Guo, Y., and Ye, J. Object detection in 20 years: A survey. *Proceedings of the IEEE*, 111(3):257–276, 2023.

Appendix

We provide more details and experiments of this work in the appendix and organize them as follows:

- Appendix A: we conduct a statistical analysis on the length of detection information, showcasing the efficacy of our compression strategy.
- Appendix B: we provide examples on which LLaVA-1.5-13B fails while our model LAF-13B with detection information succeeds.
- Appendix C: we provide examples of images along with their corresponding detection information, showing how the detection information is constructed.
- Appendix D: we introduce the instruction-following dataset of LLaVA-1.5.
- Appendix E: we summarize the training hyperparameters for our training strategy.
- Appendix F: we present benchmark scores for LAR models and LAF models on MME-Perception and MME-Cognition.
- Appendix G: we fine-tune another version on LLaVA-1.5 without the addition of detection information. The results indicate that the exceptional performance of LAF models is primarily ascribed to the supplementary detection information, rather than the additional fine-tuning conducted on LLaVA-1.5.
- Appendix H: we assess the performance of LAF models without incorporating any detection information, affirming that the LAF fusion strategy proficiently harnesses the features extracted from ViT.
- Appendix I: we show the performance of LAF models exclusively utilizing OCR information or object detection information, affirming that they can respectively enhance the performance of our model on relevant tasks.

A. Length of Detection Information

Since the textual descriptions of bounding box coordinates typically involve a lot of digits, their token sequences are often long. We devise strategies to succinctly represent the spatial information of detected objects and texts, mitigating the verbosity of bounding box descriptions. By focusing on central coordinates and consolidating objects within the same category, we maintain brevity and clarity in our model’s inputs.

	Average length	Average length (excluding 0)
Object Detection	118.5	125.1
OCR	29.4	97.5

Table 5. The average sequence length of detection information.

We conduct a statistical analysis on the length of detection information using samples from the instruction-following dataset of LLaVA-1.5. According to the table, the average length of object detection information is 118.5, and the average length of OCR information is 29.4. After excluding the empty sequences, the average length of object detection information falls to 125.1, while the mean length of OCR information becomes 97.5. Consequently, these numbers fall in an acceptable range and will not excessively impact the training efficiency.

Furthermore, we notice that the maximum length for object detection information is 1,247, whereas for OCR information, the number is 3,995. Additionally, it is observed that approximately 0.6% of object detection information exceeds a length of 512, whereas about 0.2% of OCR information surpasses the 512 threshold. In other words, our compression strategy has effectively mitigated the occurrence of lengthy sequences.

Finally, to ensure the length of the input sequence does not exceed the maximum context window length of LLM, we exclude object detection or OCR information that exceeds a length of 1,024.

B. Examples on which LLaVA-1.5-13B fails while LAF-13B with detection information succeeds.

Table 5 presents examples where LLaVA-1.5 provides incorrect responses, while our LAF-13B delivers accurate answers. The showcased examples encompass scenarios related to object counting, object detection, and text recognition.










 <p>Q: How many breads are there in the picture? LLaVA-1.5-13B: There are three breads in the picture. LAF-13B: There are four breads in the picture.</p>	 <p>Q: What is the time in this picture? LLaVA-1.5-13B: The time in this picture is 12:00. LAF-13B: The time in this picture is 11:10.</p>	 <p>Q: What is the car number for the blue car? LLaVA-1.5-13B: The car number for the blue car is 547. LAF-13B: The car number for the blue car is 87925.</p>
 <p>Q: How many people are there in the image? LLaVA-1.5-13B: There are six people in the image. LAF-13B: There are eight people in the image.</p>	 <p>Q: Are there potted plants? Where are them? LLaVA-1.5-13B: Yes, there are potted plants in the image. They are located on the floor, near the girl and the open closet. LAF-13B: Yes, there are potted plants in the image. They are located on the left side of the room, near the bed.</p>	 <p>Q: What is written on the jersey of the player with number zero? LLaVA-1.5-13B: The jersey of the player with number zero reads "Stanford". LAF-13B: The jersey of the player with number zero has "TITANS" written on it.</p>
 <p>Q: Count the number of sheep in this picture. LLaVA-1.5-13B: There are five sheep in this picture. LAF-13B: There are six sheep in this picture.</p>	 <p>Q: Find the person in the picture. LLaVA-1.5-13B: There is no person visible in the image. The scene shows a street with cars parked along the sidewalk, and a traffic light is present. LAF-13B: There is a person standing on the sidewalk near the parked cars in the image.</p>	 <p>Q: What is the number of the player holding the rugby? What is the number of the black team player chasing him? LLaVA-1.5-13B: (...)The black team player chasing him is wearing the number 9. LAF-13B: (...)The black team player chasing him is number 95.</p>

Figure 5. Examples on which LLaVA-1.5-13B fails while our model with detection information (LAF-13B) succeeds

C. Examples of Detection Information



Figure 6. Examples of detection information generated with DINO and PaddleOCRv2.

D. LLaVA-1.5’s Instruction-following Dataset

The instruction-following dataset of LLaVA-1.5 (Liu et al., 2023a) is a combination of several datasets that relate to various tasks. Among them, the LLaVA dataset (Liu et al., 2023b) and ShareGPT dataset (Chiang et al., 2023) contain high-quality GPT-4 conversation data. VQAv2 (Goyal et al., 2017) and GQA (Hudson & Manning, 2019) are widely used VQA datasets, with samples requiring one word or a short phrase to answer visual questions. OKVQA (Marino et al., 2019) and A-OKVQA (Schwenk et al., 2022) are VQA datasets that aim to expand the knowledge base of multimodal models based on external prior knowledge. OCRVQA (Mishra et al., 2019) is designed to enhance the text recognition capabilities of multimodal models. TextCaps (Sidorov et al., 2020) is an image captioning dataset, where samples are in the form of one-sentence descriptions of images. RefCOCO (Kazemzadeh et al., 2014) and VG (Krishna et al., 2017) are object detection datasets designed to improve the object localization capabilities of multimodal models.

This dataset, especially with its object detection and OCR data, enables our model to better harness the additional detection information through the newly trained MLP and LoRA modules.

E. Training Hyperparameters

Hyperparameter	Pretrain-LAR	Finetune-LAR	Finetune-LAF
batch size	256	128	128
MLP lr	1e-3	2e-5	-
lr schedule		cosine decay	
lr warmup ratio		0.03	
optimizer		AdamW	
lora rank	-	128	128
lora alpha	-	256	256
lora lr	-	2e-4	2e-4

Table 6. Hyperparameters of the second and the third experiment.

In Table 6, we show the training hyperparameters employed in our experiments. Specifically, the term “Pretrain-LAR” denotes the hyperparameters utilized during the pretraining phase for vision-language alignment in the context of the LAR fusion strategy. Similarly, “Finetune-LAR” refers to the hyperparameters employed for the subsequent fine-tuning phase focused on visual instruction tuning for the LAR fusion strategy. Additionally, “Finetune-LAF” designates the hyperparameters utilized during the fine-tuning process for the LAF fusion strategy.

Method	MME-Perception	MME-Cognition
BLIP-2	1293.8	290.0
InstructBLIP	1212.8	291.8
LLaMA-AdapterV2	1328.4	356.4
Qwen-VL-Chat	1487.5	360.7
SPHINX	1476.1	322.2
LLaVA-1.5-7B	1510.7	355.7
LAR-7B	1454.5	412.0
LAF-7B	1482.7	397.9
LLaVA-1.5-13B	1531.3	295.4
LAR-13B	1491.2	409.6
LAF-13B	1555.1	365.4

Table 7. Comparison with SOTA MLLMs on MME benchmarks.

F. MME Benchmark in Table 4

In Table 7, benchmark scores for LAR models and LAF models on MME-Perception and MME-Cognition are presented. The data in the table reveals a significant enhancement in scores for both models specifically on MME-Cognition. This notable enhancement can be ascribed to the inclusion of supplementary OCR information in our models, addressing a multitude of questions within MME-Cognition that pertain to textual content embedded within images.

Furthermore, concerning the MME-Perception benchmark, our models exhibit some fluctuations in scores. Nonetheless, it is noteworthy that the scores for LAF models surpass those for LAR models, which underscores that our third fusion approach better preserves the original capabilities of MLLM.

G. Fine-tuning on LLaVA-1.5 without Detection Information

Method	VQA ^{v2}	GQA	VQA ^T	POPE	MME ^P
LAF-7B	79.0	60.5	60.1	88.9	1482.7
LAF-7B-T w/o DI	78.2 ↓	60.5	58.2 ↓	86.8 ↓	1493.0 ↑
LAF-13B	80.3	62.2	61.8	88.8	1555.1
LAF-13B-T w/o DI	79.4 ↓	61.9 ↓	60.8 ↓	87.1 ↓	1509.0 ↓
	MME ^C	MMB	MMB ^{C/N}	MM-Vet	SEED
LAF-7B	397.9	67.3	60.2	35.2	60.8
LAF-7B-T w/o DI	345.0 ↓	67.3	60.6 ↑	29.8 ↓	60.3 ↓
LAF-13B	365.4	71.4	65.2	38.9	62.3
LAF-13B-T w/o DI	315.4 ↓	71.0 ↓	63.9 ↓	36.1 ↓	62.8 ↑

Table 8. If we finetune LLaVA-1.5 without detection information, the performance will be inferior to the version with detection information. -T w/o DI stands for “training without detection information.”

In the third fusion strategy, our model undergoes an additional epoch of fine-tuning on LLaVA-1.5. To guarantee the fairness of the results, we fine-tune another version of

LLaVA-1.5 without the addition of detection information. In this way, we can investigate whether the performance improvement of the model is attributable to the supplementary detection information or to the fine-tuning of an additional epoch.

As indicated in Table 8, the performance of the version without detection information is on par with LLaVA-1.5. Compared to our model, this model exhibits inferior performance across all benchmarks. Consequently, the outstanding performance of our LAF models is more attributed to the detection information we supplement, rather than that we fine-tune for an extra epoch on LLaVA-1.5.

H. Analysis of LAF models without Detection Information

Method	VQA ^{v2}	GQA	VQA ^T	POPE	MME ^P
LLaVA-1.5-7B	78.5	62.0	58.2	85.9	1510.7
LAR-7B w/o DI	76.4	56.8	56.6	85.5	1387.7
LAF-7B w/o DI	78.0	60.7	57.1	86.0	1441.8
LAF-7B	79.0	60.5	59.8	88.9	1482.7
	MME ^C	MMB	MMB ^{CN}	MM-Vet	SEED
LLaVA-1.5-7B	355.7	64.3	58.3	30.5	58.6
LAR-7B w/o DI	312.5	65.5	58.3	29.0	59.6
LAF-7B w/o DI	303.6	66.9	59.7	30.1	60.6
LAF-7B	397.9	67.3	60.2	35.2	60.8

Method	VQA ^{v2}	GQA	VQA ^T	POPE	MME ^P
LLaVA-1.5-13B	80.0	63.3	61.3	85.9	1531.3
LAR-13B w/o DI	77.3	58	58.2	83.4	1442.6
LAF-13B w/o DI	79.4	62.1	60.0	85.3	1525.7
LAF-13B	80.3	62.2	61.8	88.8	1555.1
	MME ^C	MMB	MMB ^{CN}	MM-Vet	SEED
LLaVA-1.5-13B	295.4	67.7	63.6	35.4	61.6
LAR-13B w/o DI	310.7	68.5	61.7	30.6	61.6
LAF-13B w/o DI	320.0	70.8	64.8	36.0	61.7
LAF-13B	365.4	71.4	65.2	38.9	62.3

Table 9. If we do not append detection information to LAF models during inference, its performance will be on par with LLaVA-1.5. “w/o DI” is an abbreviation for “without detection information.”

We assess the benchmark scores of LAF models without detection information, to evaluate their capacities in leveraging ViT features. The findings delineated in Table 9 demonstrate that the efficacy of LAF-NDI models aligns closely with that of LLaVA-1.5, and they outperform LAR-NDI models across all benchmarks. This implies that our third fusion strategy effectively empowers the model to assimilate and capitalize on information extracted by ViT.

I. Performance of LAF models exclusively with OCR Information or Object Detection Information

Method	VQA ^{v2}	GQA	VQA ^T	POPE	MME ^P
LAF-7B-NDI	78.0	60.7	57.1	86.0	1441.8
LAF-7B-OCR	78.3 ↑	60.6	60.3 ↑	86.1	1454.4 ↑
LAF-13B-NDI	79.4	62.2	60.0	85.3	1525.7
LAF-13B-OCR	79.7 ↑	62.2	61.8 ↑	85.4	1556.9 ↑
	MME ^C	MMB	MMB ^{CN}	MM-Vet	SEED
LAF-7B-NDI	303.6	66.9	59.7	30.1	60.6
LAF-7B-OCR	399.3 ↑	66.7	59.5	35.1 ↑	60.5
LAF-13B-NDI	320.0	70.9	64.8	36.0	61.7
LAF-13B-OCR	367.5 ↑	71.1	65.0	38.0 ↑	61.9

Table 10. Performance of LAF models only with OCR information.

Method	VQA ^{v2}	GQA	VQA ^T	POPE	MME ^P
LAF-7B-NDI	78.0	60.7	57.1	86.0	1441.8
LAF-7B-DINO	79.0 ↑	60.5	57.1	89.0 ↑	1469.2 ↑
LAF-13B-NDI	79.4	62.2	60.0	85.3	1525.7
LAF-13B-DINO	80.0 ↑	62.2	60.1	89.0 ↑	1529.7 ↑
	MME ^C	MMB	MMB ^{CN}	MM-Vet	SEED
LAF-7B-NDI	303.6	66.9	59.7	30.1	60.6
LAF-7B-DINO	302.1	67.2 ↑	60.2 ↑	31.5 ↑	61.0 ↑
LAF-13B-NDI	320.0	70.9	64.8	36.0	61.7
LAF-13B-DINO	317.9	71.1 ↑	65.0 ↑	37.0 ↑	62.3 ↑

Table 11. Performance of LAF models only with object detection information.

As evident from Table 10 and Table 11, the inclusion of object detection information significantly boosts the scores of relevant benchmarks for object localization and object hallucination. Similarly, the incorporation of OCR information markedly improves the scores of benchmarks related to text recognition.